Direct Qualitative Analysis of Triacylglycerols by Electrospray Mass Spectrometry Using a Linear Ion Trap

Andrew M. McAnoy, Christine C. Wu, and Robert C. Murphy
Department of Pharmacology, University of Colorado at Denver and Health Sciences Center, Aurora, Colorado, USA

Triacylglycerols (TAGs) isolated from a biological sample provide a challenge for mass spectrometric analysis because of the complexity of naturally occurring TAGs, which may contain different fatty acyl substituents resulting in a large number of molecular species having the identical elemental composition. We have investigated the use of mass spectrometry to obtain unambiguous information as to the individual TAG molecular species present in a complex mixture of triacylglycerols using a linear ion trap mass spectrometer. Ammonium adducts of TAGs, $[M + NH_4]^+$, were generated by electrospray ionization, which permitted the molecular weight of each TAG molecular species to be determined. The mechanisms involved in the decomposition of the $[M + NH_4]^+$ and subsequent fragment ions were investigated using deuterium labeling, MS/MS, and MS^3 experiments. Collision induced decomposition of $[M + NH_4]^+$ ions resulted in the neutral loss of NH_3 and an acyl side-chain (as a carboxylic acid) to generate a diacyl product ion. MS/MS data were used to identify each acyl group present for a given $[M + NH_4]^+$ ion, and this information could be combined with molecular weight data to identify possible TAG molecular species present in a biological extract. Subsequent MS^3 experiments on the resultant diacyl product ions, which gave rise to acylium (RCO^+) and related ions, enabled unambiguous TAG molecular assignments. These strategies of MS, MS/MS, and MS^3 experiments were applied to identify components within a complex mixture of neutral lipids extracted from RAW 264.7 cells. (J Am Soc Mass Spectrom 2005, 16, 1498–1509) © 2005 American Society for Mass Spectrometry

Triacylglycerols (TAGs) are relatively simple lipid substances in that they are made up of free fatty acids esterified to the 3-carbinol oxygen atoms of glycerol. In spite of their being glycerol triesters, these fat molecules are at the center of some of the most complex biochemical systems that drive energy production and storage in an organism [1]. Since these molecules are essentially water insoluble, a transport mechanism is required for their movement in the blood and distribution to distal cells. This is accomplished by the family of lipoproteins such as chylomicrons, very low density lipoproteins (VLDL), and to some extent, low density lipoproteins (LDL) [2, 3]. These soluble complexes of various physical sizes deliver TAGs to virtually every cell in the body. At the cellular site, hormone sensitive lipase rapidly degrade TAGs to free fatty acids and glycerol either for energy production, biochemical intermediate metabolism, or reconversion to TAGs for storage [4]. Evidence has been accumulating that the extraordinary rise in Type II diabetes, in particular with individuals below the age of 30, is directly or indirectly related to elevation of TAGs in the diet [5, 6].

Triacylglycerols are present in all cells in various amounts with the adipocyte being the cell with the largest quantity, since it is a specialized cell for the storage of this type of lipid [7]. Also, there is evidence that cells can transport TAGs from intracellular lipid bodies to the cell membrane by means of an intracellular organelle called the adiposome [8]. TAGs exist as unique molecular species of lipids within cells, and the analysis of these lipids present considerable challenge to the analytical biochemist. Much of our present understanding of the role of TAGs comes from measurement of either the total quantity of TAG present in cells or fatty acids that can be released from TAGs after isolation and saponification, rather than knowledge of TAG molecular species. GC/MS and electron ionization was employed to assess the complexity of naturally occurring TAG molecular species as early as the 1970s, exemplified by the work of Hites and coworkers [9–11]. However, the volatility of some TAGs, especially those containing polyunsaturated fatty acyl groups, require very high temperatures (>300 °C) to elute from a gas chromatograph, which can lead to decomposition in the well known ester pyrolysis reaction. More recently, electrospray ionization and atmospheric pressure ion-

Published online July 12, 2005

Address reprint requests to Dr. R. C. Murphy, Department of Pharmacology, University of Colorado Health Sciences Center, Mail Stop 8303, P.O. Box 6511, Aurora, CO 80045-0511, USA. E-mail: robert.murphy@uchsc.edu

1044-0305/05/$30.00
doi:10.1016/j.jasms.2005.04.017

Received March 4, 2005
Revised April 25, 2005
Accepted April 27, 2005

ization have been employed to analyze TAGs at the molecular species level using considerably gentler conditions°[12–15].°Notable°advances°were°made°by°Han and°Gross°[16]°and°Hsu°and°Turk°[17]°using°lithium adducts of TAGs with collisional activation of the $[M + Li]^+$ ions to yield diacyl product ions that revealed specific information about acyl groups esterified to individual TAG molecular species. Also, Byrdwell and Neff employed MS^3 to study the composition of synthetic°TAG°species°[18].°Cheng,°Gross,°and°Pittenauer used high-energy collisions of ammonium and sodium adducts of TAGs to elucidate acyl position on the glycerol backbone and double-bond location of unsaturated°acyl°moieties°[19]°of°pure°TAG°molecular°species.

The potential complexity of TAG molecular species derived from biological sources can be illustrated by calculating the theoretical number of unique species that can be derived from the common, naturally occurring fatty acyl groups found in cells originating from decanoic acid (C_{10}) to dodecanoic acids (C_{22}) including odd chain fatty acids and common unsaturated fatty acids such as oleic, linoleic, arachidonic, and docosahexaenoic acid. Such a list would include 30 different fatty acids, but would result in more than 25,000 different molecular species. While many of these are positional isomers (esterification of the same fatty acids but at different glycerol carbon atoms at sn-1, sn-2, and sn-3), the total number of unique species (differing by different fatty acyl substituents) is still enormous. For example, there are 129 species that could result in a $[M + NH_4]^+$ adduct ion at *m/z* 878.8 (±0.1) and 43 of those have unique esterified fatty acids at this single mass-to-charge ratio.

We describe here a strategy using MS^3 to analyze TAGs from a complex mixture as the NH_4^+ adduct ions using electrospray ionization. This method was used to unambiguously identify the unique molecular species at the level of individual esterified fatty acyl groups present within the RAW 264.7 cells.

Materials and Methods

Materials

Triacylglycerol standards glyceryl 1,2-dipalmitate-3-stearate (16:0/16:0/18:0) and glyceryl 1,2-dipalmitate-3-oleate (16:0/16:0/18:1) were obtained from Avanti Polar Lipids (Alabaster, AL). Labeled triacylglycerols glyceryl-1,1,2,3,3-D_5 trihexadecanoate, 98% (D_5-tripalmitin) and glyceryl tri(hexadecanoate-2,2-D_2), 98% (D_6-tripalmitin) were purchased from C/N/D isotopes (Pointe-Claire, Quebec, Canada). Glyceryl trioleate (18:1/18:1/18:1), ammonium-D_4 acetate-D_3, 98%, methanol-OD, 99.5% and deuterium oxide (D_2O), 99.9% were purchased from Aldrich (Milwaukee, WI). All solvents were HPLC-grade and obtained from Fisher Scientific (Fair Lawn, NJ). Discovery DSC-NH_2 amino propyl solid-phase extraction columns (3 mL tube, 500 mg) were purchased from Supelco (Bellefonte, PA).

Cells

The cells used in this study were the RAW 264.7 macrophage-like cell line derived from tumors induced in male BALB/c mice by the Abelson murine leukemia virus. The RAW 264.7 cells were obtained from ATCC laboratories (cat. no. TIB-71; lot no. 3002360) for use by the LIPID MAPS consortium. In brief, the cells were grown in an incubator with a 5% CO_2, humidified atmosphere maintained at 37 °C. Cells were allowed to grow until 80% confluent (2 to 3 days) at which time they were passed and/or harvested. Passage involved dispensing 5×10^6 cells into a new 150 cm^3 flask with fresh medium.

Extraction and Isolation of Neutral Lipids

Lipids were extracted from the RAW 264.7 cells using the°Bligh-Dyer°method°[20].°TAGs°were°then°separated from the lipid extract as part of the neutral lipid fraction by° a° solid-phase° extraction° method° [21].° Briefly,° the lipid extract from 1×10^8 cells was added to an amino propyl column (Supelco DSC-NH_2, 3 mL tube, 500 mg) previously equilibrated with hexane (9 mL) before loading the lipid extract dissolved in chloroform (200 μL). A mixture of chloroform:isopropanol (2:1, 6 mL) was then used to elute the neutral lipids. The neutral lipid fraction was then dried under nitrogen and redissolved in $CHCl_3$ (1 mL) and stored at −20 °C.

Preparation of Samples for Mass Spectrometric Analysis

An aliquot (100 μL) of the neutral lipid fraction was diluted in 900 μl chloroform:methanol (1:1, vol/vol) and 20 μL aqueous NH_4OAc (0.1 M) was then added, resulting in a final ammonium ion concentration of 5 mM. TAG standard ESI mixtures were prepared in an identical solvent system at a concentration of 10 ng/μL. ESI mixtures for experiments involving active hydrogen atom exchange of the ammonium ion were prepared using aqueous ammonium-D_4 acetate-D_3 (98%, 0.1 M in D_2O, 99.9%) and methanol-OD, 99.5%.

Electrospray Ionization Mass Spectrometry (ESI/MS)

ESI mass spectrometry was carried out using a Thermo-Finnigan LTQ linear ion trap mass spectrometer (San Jose, CA) equipped with an electrospray ionization source. The sample was introduced into the ESI source directly, via a drawn microcapillary, at a rate of 1.0 μl/min. The mass spectrometer was operated in positive ESI mode and the signal tuned for the transmission and detection of TAG ammonium adduct ions. Typical

Table 1. MS/MS data of the $[M+NH_4]^+$ ions from various labeled TAGs and corresponding observed mass-to-charge ratio of the diacyl product ion

TAG Ion	Molecular adduct (*m/z*)	Diacyl product ion (*m/z*)	Neutral loss (amu)[1]
$[16:0/16:0/16:0]NH_4^+$	824	551	273
$[D_6\text{-}16:0/16:0/16:0]NH_4^+$	830	555	275
$[D_5\text{-}16:0/16:0/16:0]NH_4^+$	829	556	273
$[16:0/16:0/16:0]ND_4^+$	828	551	277
$[16:0/16:0/18:0]NH_4^+$	852	579, 551	273, 301
$[16:0/16:0/18:0]ND_4^+$	856	579, 551	277, 305
$[16:0/16:0/18:1]NH_4^+$	850	577, 551	271, 299
$[16:0/16:0/18:1]ND_4^+$	854	577, 578, 551	277, 276, 303
$[18:1/18:1/18:1]NH_4^+$	902	603	299
$[18:1/18:1/18:1]ND_4^+$	906	603, 604	303, 302

[1]Calculated mass loss of the molecular adduct, corresponding to the loss of NH_3 and a carboxylic acid, to produce the observed diacyl product ion in the MS/MS spectrum.

experimental conditions were as follows; source voltage, 2.40 kV; capillary temperature, 250 °C; capillary voltage, 29.0 V; ion isolation window, 1.5 u; maximum ion inject time, 100 ms; collision energy (MS^2), 30% and collision energy (MS^3), 25%. ESI/MS spectra were averaged over 50 scans, while MS/MS and MS^3 scans were collected for 0.5 min and spectra averaged over ~100 scans.

A mass shift of the precursor TAG molecular adduct was observed during MS/MS scans, such that centering on the mass of interest gave substantial isotopic interference. This was investigated further by stepping over the mass range *m/z* 822–826 in 0.2 u increments and recording the MS/MS spectrum at each *m/z* value. The most intense MS/MS spectra over this range were found to correspond to the TAGs [^{13}C]48:2, 48:1, [^{13}C]48:1, and 48:0 at *m/z* 822.7, 823.5, 824.5, and 825.7, respectively, equating to an average mass shift of 0.9 u. This mass shift was also observed using TAG standards, 16:0/16:0/18:0 (*m/z* 850) and 16:0/16:0/18:1 (*m/z* 852), both combined and separately. We therefore corrected for this phenomenon in all our MS^n experiments using the empirical mass shift of 0.9 u.

Results

MS/MS of Labeled TAGs

The collision induced decomposition (CID) of TAG ammonium adduct ions $[M + NH_4]^+$ resulted in the characteristic loss of the elements of RCOOH and NH_3 as previously described [18, 19], and a small but real $[M + H]^+$ corresponding to the loss of NH_3. While we typically observed relative ion abundances from 1 to 5%, other investigators using the 3-D ion trap have observed abundances up to 20% [18]. A number of structures for the resultant diacyl product ion have been suggested [15, 19], but no extensive mechanistic study has been reported for this abundant ion. Therefore, a series of experiments with deuterium labeled TAGs were conducted to determine the mechanism of diacyl product ion formation in the MS/MS spectra of ammoniated adducts (Table 1). A similar study of deuterium labeled lithiated TAGs revealed that an analogous carboxylic acid loss resulted from a complicated mechanism involving the abstraction of an α-methylene proton from the acyl side-chain [17].

Collision induced decomposition of the $[M + NH_4]^+$ ion of (unlabeled) tripalmitin (*m/z* 824) resulted in a diacyl product ion at *m/z* 551 (Figure 1a). This observed loss of 273 u corresponded to the combined loss of $CH_3(CH_2)_{14}COOH$ and NH_3. CID of the $[M + NH_4]^+$ ion of D_6-tripalmitin (*m/z* 830), where all six α-methylene hydrogen atoms are replaced with deuterium atoms, underwent a neutral loss of 275 u corresponding to

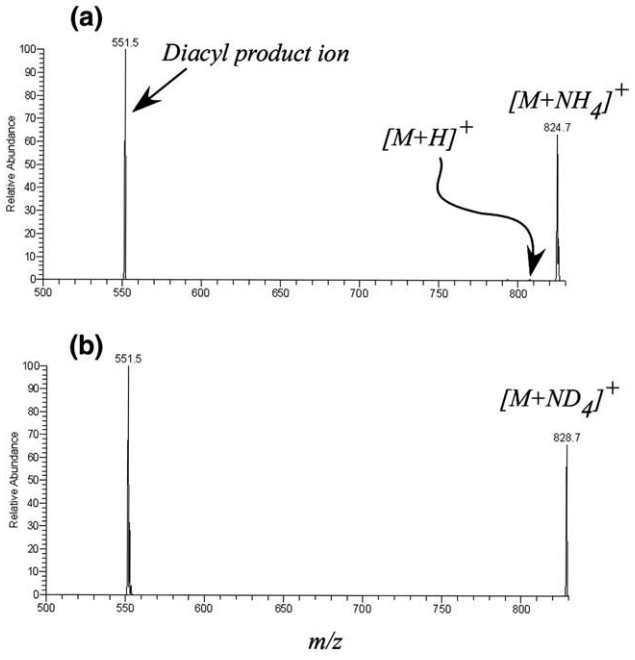

Figure 1. MS/MS spectra of (**a**) *m/z* 824 $[M + NH_4]^+$ from a mixture of tripalmitin (10 ng/μL) in $CHCl_3$:MeOH (1:1) with 5 mM NH_4OAc, and (**b**) *m/z* 828 $[M + ND_4]^+$ from a mixture of tripalmitin (10 ng/μL) in $CHCl_3$:MeOD (1:1) with 5 mM ND_4OAc, obtained on a LTQ mass spectrometer.

Table 2. MS^3 data from unlabeled and labeled tripalmitin ammonium adducts[1]

TAG ion	MS/MS fragment ion (*m/z*)	RCO^+ (*m/z*)	$[RCO + 74]^+$ (*m/z*)
$[16:0/16:0/16:0]NH_4^+$	551	239	313
$[D_5\text{-}16:0/16:0/16:0]NH_4^+$	556 (+5)	239	318 (+5)
$[D_6\text{-}16:0/16:0/16:0]NH_4^+$	555 (+4)	241 (+2)	316 (+3)

[1]Observed mass shift of ions from labeled tripalmitin compared to the unlabeled tripalmitin is indicated in parenthesis.

the combined loss of $CH_3(CH_2)_{13}CD_2COOH$ and NH_3, indicating that an α-methylene hydrogen atom was not involved in the carboxylic acid loss. It was possible that this process involved a hydrogen atom on the glycerol backbone which might be abstracted by a carboxyl oxygen via a six-membered cyclic intermediate. If the process was active in the decomposition of tripalmitin, the neutral loss from the $[M + NH_4]^+$ ion of D_5-tripalmitin (*m/z* 829), where all five hydrogen atoms on the glycerol backbone are replace with deuterium atoms, would be mass shifted to 274 u to reflect the combined loss of $CH_3(CH_2)_{14}COOD$ and NH_3. However, the observed neutral loss of 273 u corresponded to the loss of $CH_3(CH_2)_{14}COOH$ and NH_3, indicating that the glycerol hydrogen atoms were not involved the acyl side-chain loss. At this stage, the only remaining hydrogen atoms likely to be involved in the acyl side-chain loss from ammoniated TAGs originated from the ammonium ion itself. Labeling of the ammonium hydrogen atoms was therefore carried out through active hydrogen atom exchange conditions and the $[M + ND_4]^+$ ion of (unlabeled) tripalmitin (*m/z* 828) was observed to undergo a neutral loss of 277 u (Figure 1b), consistent with the combined loss of $CH_3(CH_2)_{14}COOD$ and ND_3 to form the product ion at *m/z* 551. The ion observed at *m/z* 552 (Figure 1b) was due to the presence of the ^{13}C isotope from the $[M + ND_3H]^+$ ion present at *m/z* 828.8 from incomplete H–D exchange. Correcting for contribution to the ion observed at *m/z* 551 (Figure 1b) attributable to the ^{13}C-$[M + ND_3H]^+$ ion indicates that greater than 85% of the total ion abundance of *m/z* 551 was indeed due to loss of $CH_3(CH_2)_{14}COOD$ and ND_3 from the $[M + ND_4]^+$ ion. This result strongly supported an ammonium ion origin for the carboxylate proton in the palmitic acid, which was lost in the decomposition of ammoniated tripalmitin.

To further investigate the mechanism involved in the decomposition of $[M + NH_4]^+$ derived from TAGs, additional ND_4^+ labeled studies were carried out using TAG standards 16:0/16:0/18:0, 16:0/16:0/18:1, 18:1/18:1/18:1 (Table 1). In each case, neutral losses from the labeled ND_4^+ adducts were mass shifted by 4 u in comparison with the unlabeled NH_4^+ adducts, consistent with the involvement of the ammonium hydrogen atoms. For example, the neutral loss of the acyl side-chain 18:1 plus ammonia from the ND_4^+ adduct of 16:0/16:0/18:1 (*m/z* 854), which resulted in a diacyl product ion without acyl double bonds (*m/z* 551), was found to mass shift from 299 to 303 u. However, the neutral acyl losses which formed the unsaturated diacyl product ions, 16:0/18:1 (*m/z* 577 and 578) and 18:1/18:1 (*m/z* 603 and 604), from the ND_4^+ adducts of 16:0/16:0/18:1 (*m/z* 854) and 18:1/18:1/18:1 (*m/z* 906), were observed to be mass shifted by both 3 and 4 u, most likely corresponding to losses of $(RCOOH + ND_3)$ and $(RCOOD + ND_3)$ in competing processes.

The dissociation of diacyl product ions formed from TAGs reported as MS^3 experiments were observed to give rise to RCO^+ and $[RCO + 74]^+$ ions, both of which underwent loss of water [18]. MS^3 experiments on the diacyl product ions from the $[M + NH_4]^+$ ions of tripalmitin, D_5-tripalmitin and D_6-tripalmitin were carried out using a LTQ mass spectrometer and the relevant product ion data is listed in Table 2. Decomposition of the diacyl product ion (*m/z* 551) from unlabeled ammoniated tripalmitin gave rise to RCO^+ (*m/z* 239) and $[RCO + 74]^+$ (*m/z* 313) ions. The corresponding resultant ions in the MS^3 spectrum of the diacyl product ion (*m/z* 556) from the D_5-palmitin ammonium adduct (*m/z* 829) were unlabeled RCO^+ (*m/z* 239) and partially labeled $[RCO + 79]^+$ (*m/z* 318), while the resultant ions in the MS^3 spectrum of the diacyl product ion (*m/z* 555) from the D_6-tripalmitin ammonium adduct (*m/z* 830) were D_2-RCO^+ (*m/z* 241) and $[D_2\text{-}RCO + 75]^+$ (*m/z* 316). Thus, the MS^3 data indicated that both α-methylene protons were retained in the acylium ions and one additional α-methylene hydrogen atom was retained in the $[RCO + 74]^+$ ion.

TAGs in RAW Cells

The neutral lipid fraction obtained from RAW 264.7 cells contained a complex mixture of TAGs with the majority of the molecular ions observed between *m/z* 800 to 950 which was a mass-to-charge window that did not overlap with any other class of neutral lipids, such as cholesterol esters, in this neutral lipid fraction (Figure 2a). The major ions observed in the spectrum corresponded to ammoniated TAGs and thus appeared at even masses with a large fractional mass attributable to the large number of hydrogen atoms [1]. No abundant ions corresponding to $[M + H]^+$ or $[M + Na]^+$ were observed in this sample. This level of ESI MS data were used to calculate the molecular weight of individual species assuming the ions corresponded to $[M + NH_4]^+$ ions of TAGs. The total number of acyl carbons and double bonds was then determined using expected fatty acyl groups, e.g., *m/z* 824 corresponded to an ammoniated TAG with 48 acyl carbons and no double bonds (48:0). An expanded mass spectrum of the neu-

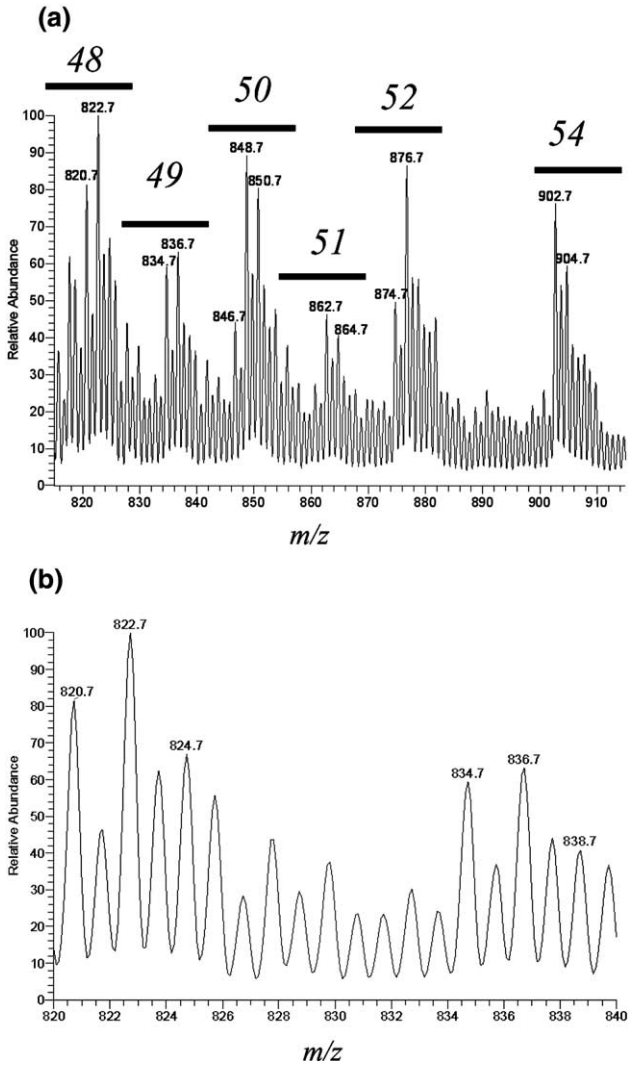

Figure 2. ESI mass spectra of the neutral lipid fraction of RAW 264.7 cells obtained on a LTQ mass spectrometer showing (**a**) the TAG region of the mass spectrum, and (**b**) the expanded *m/z* of the $[M + NH_4]^+$ corresponded to TAGs containing a total of 48 and 49 acyl carbon atoms.

tral lipid fraction (Figure 2b) revealed to some extent the complexity of the TAG mixture including species as 48:0 (*m/z* 824), 48:1 (*m/z* 822), and 48:2 (*m/z* 820). Parent ions corresponding to TAGs with an odd number of total acyl carbon atoms were also present, namely 49:0 (*m/z* 838), 49:1 (*m/z* 836), and 49:2 (*m/z* 834) (Figure 2).

Dissociation of each TAG molecular ammonium adduct ion would result in the loss of each acyl group as a neutral fatty acid and thus three, possibly distinct, diacyl product ions for each species making up the nominal $[M + NH_4]^+$ ion. When the $[M + NH_4]^+$ ions corresponding to the TAGs 48:0 (*m/z* 824), 48:1 (*m/z* 822), 48:2 (*m/z* 820), 49:0 (*m/z* 838), 49:1 (*m/z* 836), and 49:2 (*m/z* 834) were collisionally activated, (Figure 3 and Figure 4) the MS/MS yielded a large number of diacyl product ions. For example, collisional activation of *m/z* 820, which corresponded to the 48:2 TAG molecular species, yielded 10 or more diacyl product ions (Figure 3c). Each diacyl product ion could be used to identify a unique fatty acyl substituent (from the neutral loss) in the original TAG (Figures 3 and 4).

This identification of fatty acyl substituents was then assembled for each nominal mass that was collisional activated (Table 3) where columns are representative of individual TAGs in a specific mass-to-charge ratio, while rows represent the possible acyl side chains. Table 3 reflected both positive (shaded) or negative (unshaded) diacyl product ions observed corresponding to the loss of each acyl side-chain listed. For example, the MS/MS spectrum of *m/z* 824 (48:0) yielded ions at *m/z* 523, 537, 551, 565 and 579 which corresponded to the loss of the fatty acyl substituents; 18:0, 17:0, 16:0, 15:0, 14:0, respectively, but not other fatty acyl groups.

A list of possible TAG molecular species using the MS/MS data from Table 3 could then be calculated by combining the acyl chains present for each $[M + NH_4]^+$ such that the total number of carbons and double bonds

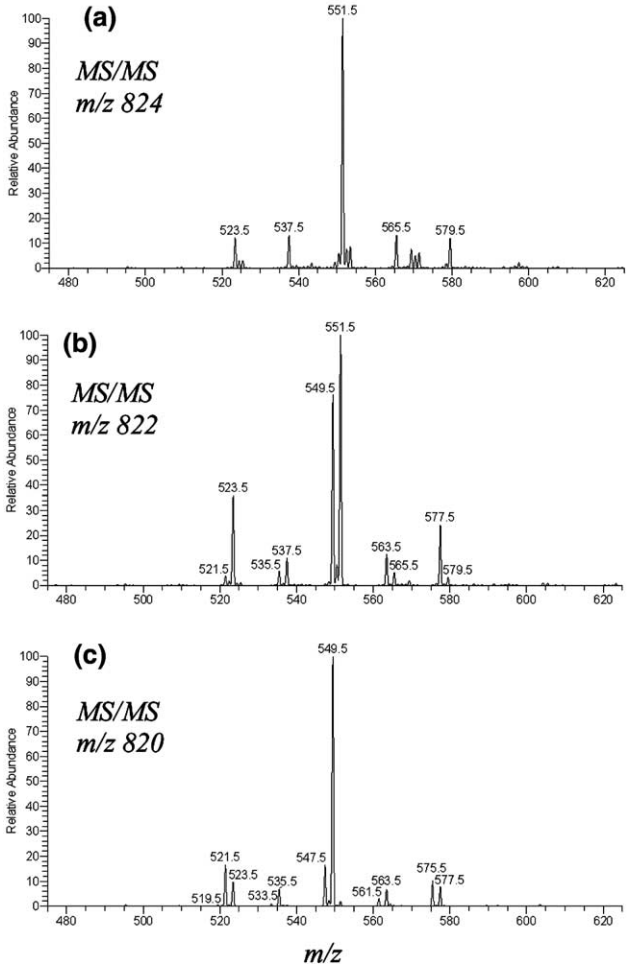

Figure 3. MS/MS spectra of (**a**) 48:0 (*m/z* 824), (**b**) 48:1 (*m/z* 822), and (**c**) 48:2 (*m/z* 820) obtained on a LTQ mass spectrometer by infusing a neutral lipid fraction of RAW 264.7 cells in $CHCl_3$:MeOH (1:1) with 5 mM NH_4OAc.

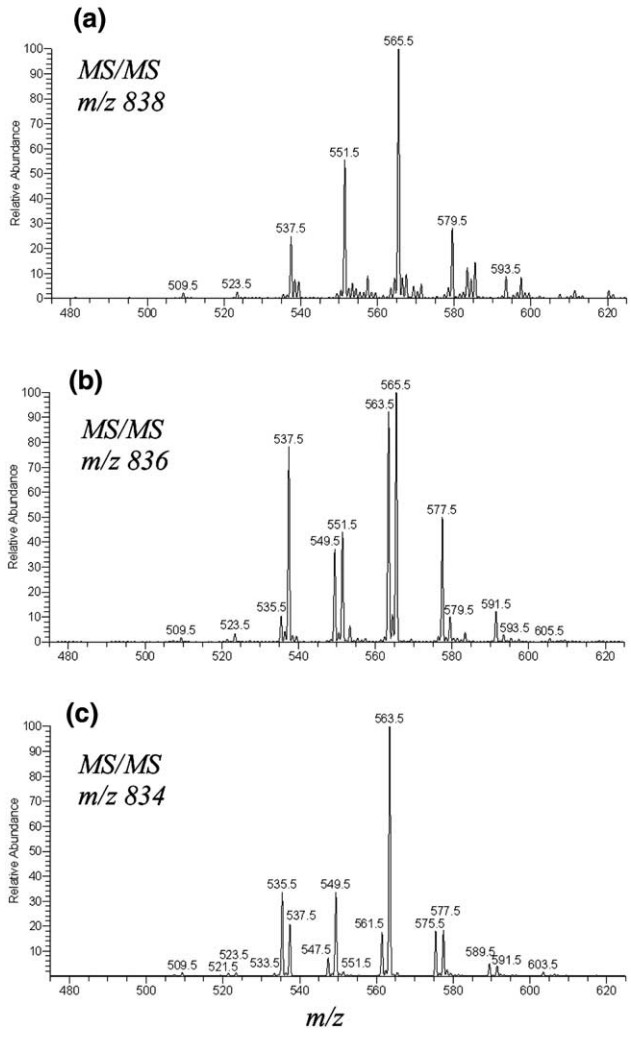

Figure 4. MS/MS spectra of (**a**) *m/z* 838 (49:0), (**b**) *m/z* 836 (49:1), and (**c**) *m/z* 834 (49:2) obtained using a LTQ mass spectrometer by infusing a neutral lipid fraction of RAW 264.7 cells in $CHCl_3$: MeOH (1:1) with 5 mM NH_4OAc.

was consistent with the molecular weight of the TAG (Table° 4).° It° should° be° noted° that° this° list° did° not distinguish between regioisomers. However, this list did include some TAG molecular species which were not present. For example, loss of acyl substituents 14:0, 15:0, 16:0, 17:0, and 18:0 from 48:0 (*m/z* 824) occurred with an approximate ratio of 1:1:10:1:1 and, given that the loss of 16:0 was much more abundant than the other acyl losses, it might be argued that the TAG species 16:0/16:0/16:0 was undoubtedly present, however there is no direct evidence for this species.

As mentioned above, the diacyl product ions from $[M + NH_4]^+$ ions of TAGs gave rise to the following ions in the MS^3 experiment: RCO^+, $[RCO - H_2O]^+$, $[RCO + 74]^+$, and $[RCO + 74 - H_2O]^+$, following an additional collisional activation and therefore the expected ions corresponding to common fatty acyl groups found in mammalian TAGs could be readily calculated°(Table°5).°Collisional°activation°of°diacyl product ions from TAGs *m/z* 824 (48:0), *m/z* 822 (48:1), *m/z* 820 (48:2), *m/z* 838 (49:0), *m/z* 836 (49:1), and *m/z* 834 (49:2) were carried out to generate the MS^3 spectra exemplified by collisional activation of the two major diacyl product ions, *m/z* 822 → 549 and 822 →°551°(Figure°5).°These°diacyl°product°ions,°*m/z* 549 and 551, would result from the respective losses of acyl moieties 16:0 and 16:1 from the 48:1 molecular species. The major ion in the MS^3 spectrum of *m/z* 822 → 549 was observed at *m/z* 313 which corresponded to the expected $[RCO + 74]^+$ for the fatty acyl 16:0 (Table° 5).° Since° the° diacyl° product° ion° (*m/z* 549) isolated for this MS^3 experiment was formed by loss of 16:0 from *m/z* 822 (48:1) and the major ion in the MS^3 spectra was due to the acyl group 16:0, the remaining acyl side-chain must be 16:1. Closer inspection° of° the° $MS^{3°}$ spectrum° (Figure° 5a)° revealed ions at *m/z* 237 and 219, which corresponded to RCO^+ and $[RCO - H_2O]^+$ ions from 16:1, confirming the diacyl pair 16:0/16:1 to make up *m/z* 549 as the diacyl product ion from *m/z* 822. In addition, the neutral loss component of this transition, *m/z* 549 → 237 was consistent with the loss of a 16:0 acyl group attached to the glycerol backbone remnant. Thus, the MS^3 data uniquely identified the TAG 16:0/16:0/16:1 in the neutral lipid fraction of RAW 264.7 cells. The assignment of the remaining ions in the MS^3 spectrum (Figure°5a)°to°diacyl°pairs°resulted°in°the°identification of isobaric TAGs; 14:0/16:0/18:1, 14:1/16:0/18:0, 15:0/16:0/17:1, and 15:1/16:0/17:1. The abundance of ions at *m/z* 211, 285, 247, 265, and 341, which arose from the diacyl pair 14:0/18:1, indicated that this diacyl pair was a significant but minor contributor to the *m/z* 549 diacyl product ion. In turn, this suggested that the TAG 14:0/16:0/18:1 was a minor component of 48:1. The abundance of the other fragment ions in this MS^3 spectrum suggested that the remaining 48:1 species could be identified as 14:1/16:0/18:0, 15:0/16:0/17:1, and 15:1/16:0/17:1, and likely were of low to trace°abundance°(Figure°5).

The most intense ion in the MS/MS spectrum of *m/z* 822°(Figure°3b)°corresponded°to°the°diacyl°product ion *m/z* 551 formed by the loss of a 16:1 fatty acyl group. Since 16:0/16:0/16:1 had already been identified as a major component of 48:1, the MS^3 spectrum of *m/z* 822 → 551 served as a check for this assignment, as well as to identify additional isobaric TAGs. As expected, the major ion in the MS^3 spectrum (Figure° 5b)° corresponded° to° the° acyl° group° 16:0, identifying the diacyl pair 16:0/16:0, and in turn indicated that the TAG 16:0/16:0/16:1 was a major component of 48:1 (*m/z* 822).

The°complete°$MS^{3°}$ data°for°the°48°and°49°carbon series°of°TAGs°can°be°summarized°(Tables°6°and°7)°as the loss of an acyl group to form a diacyl product ion, which was collisionally activated to give rise to ions characteristic of each fatty acyl substituent as observed in the MS^3 experiment and the third acyl substituent from the neutral loss in the MS^3 experi-

Table 3. Fatty acyl composition of TAG molecular species (48:0, 48:1, 48:2, 49:0, 49:1 and 49:2) extracted from RAW 264.7 cells determined using MS/MS. Acyl chains identified are indicated as a shaded entry

Acyl Chain	TAG(48:0)	TAG(48:1)	TAG(48:2)	TAG(49:0)	TAG(49:1)	TAG(49:2)
13:0					■	■
14:0	■	■	■	■	■	■
14:1		■	■		■	■
15:0	■	■	■	■	■	■
15:1		■	■		■	■
16:0	■	■	■	■	■	■
16:1		■	■		■	■
17:0	■	■	■	■	■	■
17:1		■	■		■	■
18:0	■	■	■	■	■	■
18:1		■	■		■	■
18:2			■			
19:0				■		
19:1					■	■
19:2						■
20:0				■		
20:1					■	
20:2						■

ment. In Tables 6 and 7, triacylglycerol molecular species were defined by (1) the acyl loss in the MS/MS spectrum, (2) diacyl identity from the observed MS^3 product ions, and (3) neutral mass loss from the diacyl product ion. Twelve isobaric species could be identified as present in the single $[M + NH_4]^+$ ion corresponding to 48:0 and 23 species comprising 48:1 TAG.

Discussion

The identification of TAGs from biological samples presents a challenging problem since naturally occurring mixtures of molecular species are quite complex. While approaches to separate species using HPLC are possible [18, 22, 23], a direct mass spectrometric method would preclude the added complexity of

Table 4. Possible TAG molecular species from RAW 264.7 cells consistent with fatty acyl identification from MS/MS data and molecular weight

TAG(48:0)	TAG(48:1)	TAG(48:2)	TAG(49:0)	TAG(49:1)	TAG(49:2)
14:0/16:0/18:0	14:0/16:0/18:1	14:0/16:0/18:2	14:0/15:0/20:0	13:0/16:0/20:1	13:0/16:0/20:2
14:0/17:0/17:0	14:0/16:1/18:0	14:0/16:1/18:1	14:0/16:0/19:0	13:0/17:0/19:1	13:0/17:1/19:1
15:0/15:0/18:0	14:0/17:0/17:1	14:0/17:1/17:1	14:0/17:0/18:0	13:0/18:0/18:1	13:0/18:1/18:1
15:0/16:0/17:0	14:1/16:0/18:0	14:1/16:0/18:1	15:0/15:0/19:0	14:0/15:0/20:1	14:0/15:0/20:2
16:0/16:0/16:0	14:1/17:0/17:0	14:1/16:1/18:0	15:0/16:0/18:0	14:0/16:0/19:1	14:0/16:1/19:1
	15:0/15:0/18:1	14:1/17:1/17:0	15:0/17:0/17:0	14:0/17:0/18:1	14:0/17:1/18:1
	15:0/15:1/18:0	15:0/15:0/18:2	16:0/16:0/17:0	14:0/17:1/18:0	14:0/17:0/18:2
	15:0/16:0/17:1	15:0/15:1/18:1		14:1/17:0/18:0	14:1/17:1/18:0
	15:0/16:1/17:0	15:0/16:1/17:1		15:0/15:0/19:1	14:1/17:0/18:1
	15:1/16:0/17:0	15:1/15:1/18:0		15:0/16:0/18:1	15:0/15:1/19:1
	16:0/16:0/16:1	15:1/16:0/17:1		15:0/16:1/18:0	15:0/16:0/18:2
		15:1/16:1/17:1		15:0/17:0/17:1	15:0/16:1/18:1
		16:0/16:1/16:1		15:1/16:0/18:0	15:0/17:1/17:1
				15:1/17:0/17:0	15:1/16:0/18:1
				16:0/16:0/17:1	15:1/16:1/18:0
				16:0/16:1/17:0	15:1/17:0/17:1
					16:0/16:1/17:1
					16:1/16:1/17:0

Table 5. Partial list of common fatty acyl groups found in mammalian cells and nominal masses (*m/z*) of corresponding MS^3 fragment ions

Fatty Acyl Group[1]	RCO^+	$(RCO - H_2O)^+$	$(RCO + 74)^+$	$(RCO + 74 - H_2O)^+$
12:0	183	165	257	239
13:0	197	179	271	253
14:0	211	193	285	267
14:1	209	191	283	265
15:0	225	207	299	281
15:1	223	205	297	279
16:0	239	221	313	295
16:1	237	219	311	293
17:0	253	235	327	309
17:1	251	233	325	307
18:0	267	249	341	323
18:1	265	247	339	321
18:2	263	245	337	319
19:0	281	263	355	337
19:1	279	261	353	335
20:0	295	277	369	351
20:1	293	275	367	349
20:2	291	273	365	347
20:4	287	267	361	343
20:5	285	265	359	341
22:0	309	291	383	365
22:5	299	281	373	355
22:6	297	279	371	353

[1]Total carbon atoms: number of double bonds (not counting the carboxyl group).

HPLC separation. Nevertheless, complex mixtures of isobaric TAGs, such as those found in cell extracts, result in multiple acyl side-chain losses with concomitant uncertainty in assigning TAG identities based on MS/MS data alone. This is due to the occurrence of many isobaric diacyl product ions (e.g., 16:0/16:0 and 14:0/18:0) in the CID of TAGs that cannot be unambiguously confirmed or eliminated as possible molecular species. The analysis of lithium adducts of TAGs, which are formed under ESI conditions after the addition of Li^+, have been investigated using both MS/MS and neutral loss scanning on a tandem mass spectrometer [16, 17]. However, the collision of $[TAG + Li]^+$ ions leads to two abundant product ions corresponding to $[M + Li\text{-}RCOOH]^+$ and $[M + Li\text{-}RCOOLi]^+$ for each acyl group, while CID of $[M + NH_4]^+$ yields a single product ion for each acyl group. This is a favorable property for subsequent MS^3 experiments. When the diacyl product ions from $[M + NH_4]^+$ are further dissociated, the resulting fragment ions in the MS^3 spectrum facilitate diacyl product ion identification. To meaningfully employ this previous information, an understanding of ion formation mechanisms was needed.

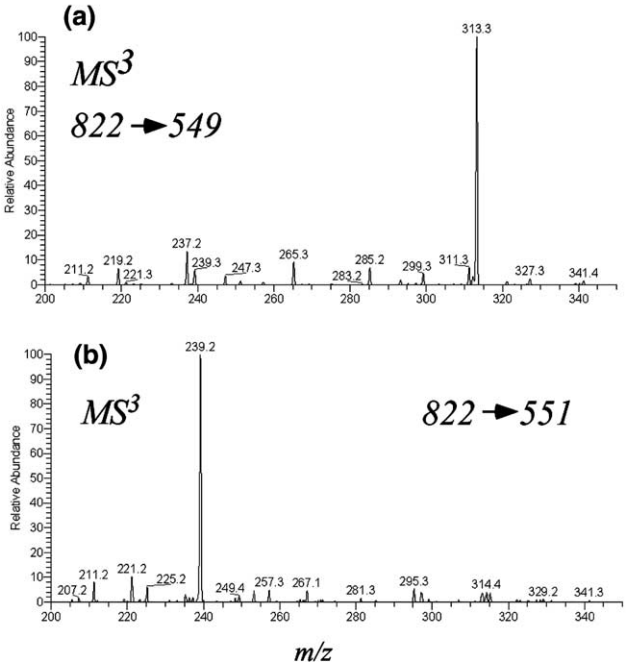

Figure 5. MS^3 spectra of major diacyl product ions (**a**) *m/z* 822 → 549 and, (**b**) *m/z* 822 → 551, obtained using a LTQ mass spectrometer by infusing a neutral lipid fraction of RAW 264.7 cells in $CHCl_3$:MeOH (1:1) with 5 mM NH_4OAc.

Possible mechanisms for the acyl side-chain loss process based on the analysis of isotope labeled species are shown in Scheme **1**, which illustrates the rearrangement of the D_5-glycerol atoms. Process A would involve the hydrogen abstraction at the sn-2 position, in a cyclic process, resulting in double-bond formation on the glycerol backbone and liberation of the sn-1/sn-3 acyl side-chain and ammonia. The resultant diacyl product ion would be protonated on the carbonyl oxygen and may then lead to the addition fragmentation in MS^3 experiments (see later discussion). The loss of the sn-2 acyl group by mechanism B would involve hydrogen abstraction at

Table 6. Summary of TAG molecular species in RAW 264.7 cells (48:0, 48:1 and 48:2) based on neutral loss of a fatty acyl group in MS/MS analysis (-Acyl column) and subsequent MS^3 acylium ions and neutral loss (diacyl pairs)[1]

TAG	- Acyl	Diacyl pairs	TAG	- Acyl	Diacyl pairs	TAG	- Acyl	Diacyl pairs
48:0	18:0 (m)	14:0,16:0 (M)	48:1	18:0 (m)	14:0,16:1 (M)	48:2	18:1 (m)	14:0,16:1 (M)
		15:0,15:0 (t)			14:1,16:0 (m)			14:1,16:0 (m)
		12:0,18:0 (t)						15:0,15:1 (t)
				18:1 (M)	14:0,16:0 (M)			12:0,18:1 (t)
	17:0 (m)	15:0,16:0 (M)			15:0,15:0 (m)			
		14:0,17:0 (t)					18:2 (m)	14:0,16:0 (M)
				17:0 (m)	15:0,16:1 (M)			15:0,15:0 (m)
	16:0 (M)	16:0,16:0 (M)			15:1,16:0 (m)			
		14:0,18:0 (m)			14:1,17:0 (t)		17:1 (m)	15:0,16:1 (M)
		15:0,17:0 (t)			14:0,17:1 (t)			15:1,16:0 (m)
								14:0,17:1 (t)
	15:0 (m)	16:0,17:0 (t)		17:1 (m)	15:0,16:0 (M)			14:1,17:0 (t)
		15:0,18:0 (t)			14:0,17:0 (t)			
							16:0 (m)	16:1,16:1 (M)
	14:0 (m)	16:0,18:0 (t)		16:0 (M)	16:0,16:1 (M)			14:1,18:1 (m)
		17:0,17:0 (t)			14:0,18:1 (m)			14:0,18:2 (t)
					15:0,17:1 (t)			
					15:1,17:0 (t)		16:1 (M)	16:0,16:1 (M)
								14:0,18:1 (m)
				16:1 (M)	16:0,16:0 (M)			15:0,17:1 (t)
					14:0,18:0 (t)			
					15:0,17:0 (t)		15:0 (m)	16:1,17:1 (t)
								15:1,18:1 (t)
				15:0 (m)	15:0,18:1 (t)			15:0,18:2 (t)
					16:0,17:1 (t)			
					16:1,17:0 (t)		15:1 (m)	15:0,18:1 (t)
				15:1 (t)	16:0,17:0 (t)		14:0 (m)	16:1,18:1 (M)
								16:0,18:2 (t)
				14:0 (m)	16:0,18:1 (M)			17:1,17:1 (t)
					16:1,18:0 (t)			
							14:1 (m)	16:0, 18:1

[1]The relative abundance of each ion and ion pair is indicated in parenthesis as M - major, m - minor, t - trace.

the sn-1/sn-3 position, in a seven centered process, resulting in double-bond formation on the glycerol backbone and an analogous loss of the sn-2 acyl side-chain and ammonia. Both mechanisms A and B were consistent with the deuterium labeled experiments of the saturated TAGs (Table 1). A lower rate of reaction for process B, compared with process A, may explain the observed lower abundance of the resultant diacyl product ions in the CID of ammoniated TAG molecular adducts [18]. However, the inference of acyl positional information based on lower diacyl product ion abundance is not straightforward [15] and the added complexity of isobaric TAG molecular species extracted from RAW 264.7 cells do not allow for such an analysis to be carried out here.

Possible mechanisms for the competing losses of RCOOH and ND_3 observed in the unsaturated TAGs are also shown in Scheme **1** as reactions C and D, which indicate the position of the D_5-glycerol atoms. These proton migrations involved a charge remote six-membered rearrangement, which resulted in the elimination of an acyl side-chain and double-bond formation on the glycerol backbone and occurred in concert with the protonation by the ammonium ion and the subsequent loss of ammonia. The ions formed by processes C and D are identical to those formed by the processes A and B, with the exception that ions C and D retain an additional deuterium label when ND_4^+ was used in the ionization process, but lose one of the glycerol hydrogen atoms as the neutral carboxylate proton (Scheme **1**).

The dissociation of the $[M + NH_4]^+$ ions of TAGs were deceptively simple in that all molecular species displayed the characteristic loss of an acyl side-chain as a neutral free acid and ammonia. Furthermore, since each of the three, possibly distinct, fatty acyl moieties could be involved in the neutral loss process, the identity of all acyl groups present in a TAG of interest could be readily determined using MS/MS data as has been published previously [16]. It follows that MS/MS data from an unknown mixture of TAGs could determine all acyl groups present in the sample. This information combined with the molecular weight of each TAG molecular species could then be used to readily characterize only pure TAGs, but not complex mixtures of isobaric TAGs.

Combined MS^3 data from labeled and unlabeled TAGs indicated that the acylium ion derived from the diacyl product ion (Scheme **1**) was generated in a

Table 7. Summary of TAG molecular species in RAW 264.7 cells (49:0, 49:1 and 49:2) based on neutral loss of a fatty acyl group in MS/MS analysis (-acyl column) and subsequent MS^3 acylium ions and neutral loss (diacyl pairs)[1]

TAG	- Acyl	Diacyl pairs	TAG	- Acyl	Diacyl pairs	TAG	- Acyl	Diacyl pairs
49:0	19:0 (t)	14:0,16:0 (M)	49:1	19:1 (t)	14:0,16:0 (M)	49:2	20:2 (t)	14:0, 15:0
		15:0,15:0 (t)			15:0,15:0 (m)			13:0, 16:0
	18:0 (m)	15:0,16:0 (M)		18:0 (m)	15:0,16:1 (M)		18:1 (m)	15:0,16:1 (M)
		13:0,18:0 (t)			15:1,16:0 (m)			15:1,16:0 (m)
					14:0,17:1 (t)			14:0,17:1 (t)
	17:0 (M)	16:0,16:0 (M)			14:1,17:0 (t)			14:1,17:0 (t)
		12:0,18:0 (t)						
				18:1 (M)	15:0,16:0 (M)		18:2 (m)	15:0,16:0 (M)
	16:0 (M)	16:0,17:0 (M)			14:0,17:0 (m)			14:0,17:0 (t)
		15:0,18:0 (m)						
				17:0 (M)	16:0,16:1 (M)		17:0 (t)	16:1,16:1 (M)
	15:0 (m)	16:0, 18:0			14:0,18:1 (m)			14:1,18:1 (m)
					14:1,18:0 (m)			15:1,17:1 (t)
				17:1 (M)	16:0,16:0 (M)		17:1 (m)	16:0,16:1 (M)
					14:0,18:0 (m)			14:0,18:1 (m)
								15:0,17:1 (t)
				16:0 (M)	15:0,18:1 (M)			
					16:0,17:1 (L)		16:0 (m)	16:1,17:1 (M)
					16:1,17:0 (L)			15:1,18:1 (m)
								15:0,18:2 (t)
				16:1 (M)	16:0,17:0 (M)			
					15:0,18:0 (m)		16:1 (M)	15:0, 18:1
					13:0,20:1 (t)			16:0, 17:1
								16:1, 17:0
				15:0 (M)	16:0, 18:1			
							15:0 (m)	16:1,18:1 (M)
				14:0 (m)	17:0, 18:1			16:0,18:2 (m)
							15:1 (m)	16:0, 18:1

[1]The relative abundance of each ion and ion pair is indicated in parenthesis as M - major, m - minor, t - trace.

simple process which involved cleavage of the carbonyl–oxygen bond. The formation of the $[RCO + 74]^+$ ion involved a rearrangement process resulting in transfer of an α-methylene hydrogen from an acyl side-chain which was concurrently eliminated as a neutral ketene. Possible mechanisms for the formation of the RCO^+ and $[RCO + 74]^+$ ions, which were consistent with the deuterium labeling experiments, are shown in Scheme **2**, where the glyceryl hydrogen atoms are labeled with deuterium and the expected mass shifts of labeled ions from D_5-tripalmitin and D_6-tripalmitin are indicated in parenthesis. The acylium ion could be formed by a 1,3-hydrogen rearrangement of the diacyl product ion (mechanism a), while the $[RCO + 74]^+$ ion formed via a cyclic process which involved abstraction of an α-methylene hydrogen atom of the diacyl product ion and elimination of an acyl side-chain as a ketene (mechanism b) (Scheme **2**). An alternative mechanism for the formation of the diacyl product ions and the $[RCO + 74]^+$ ions based on high-energy CID experiments of ammoniated TAGs°has°been°reported°[19].°This°process°involves the formation of a stable oxonium ion which may undergo elimination of an acyl side-chain as a ketene to give a $[RCO + 74]^+$ ion. The formation of the $[RCO + 74]^+$ ion from the diacyl product ion proposed in Schemes **1** and **2** is somewhat less complicated than the previous mechanism involving formation of a

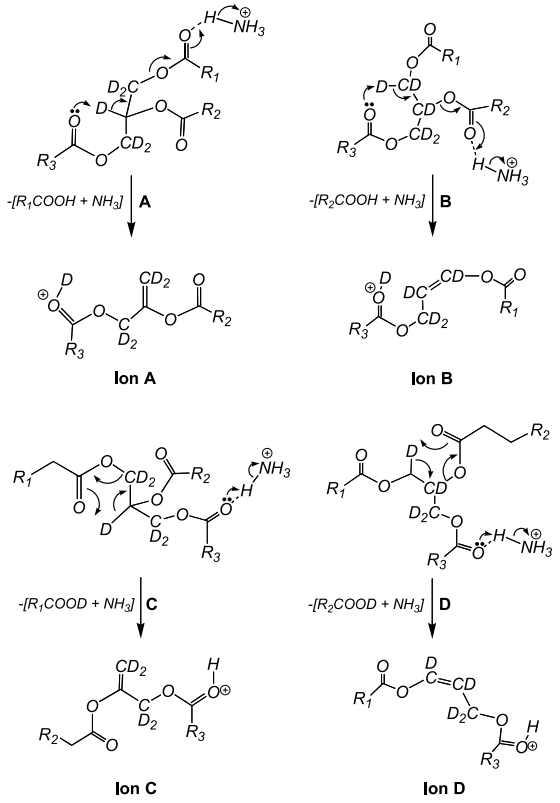

Scheme 1

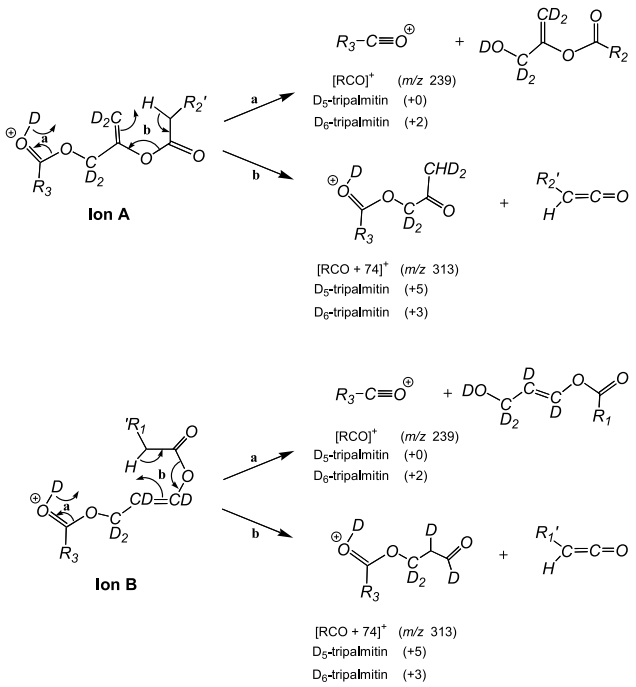

Scheme 2

protonated cyclopropane ion when ketene is lost. However, with the tools available now, these two pathways cannot be distinguished.

From just six $[M + NH_4]^+$ ions present in Figure 2a, 55 TAGs were unequivocally identified in a complex neutral lipid fraction of RAW 264.7 cells using MS^3 data (Table 8), where each TAG was classified into three arbitrary categories based on total ion abundances in the MS/MS and MS^3 spectra. Using this classification, it was determined that 56% of the TAGs were of trace abundance and were typically composed of at least one odd acyl chain. On comparing the MS/MS and MS^3 methods (Tables 4 and 8), it was noted that MS/MS only missed 4 of the 55 TAGs identified using MS^3 data and that these missed species were of trace abundance. However, the interpretation of the MS/MS data alone led to the identification of a total of 68 possible TAG molecular species, 18 of which were not identified by MS^3 experiments. Therefore, while MS/MS successfully identified 93% of the TAGs using MS^3 data, the interpretation of MS/MS results led to a list of TAGs containing up to 26% incorrectly assigned TAG molecular species. While TAGs of major abundance would likely be correctly identified using MS/MS data, it appeared difficult to distinguish between TAGs which were of minor or trace abundance, or possibly absent, in a complex biological extract using MS/MS data alone.

In conclusion, the mechanisms involved in the decomposition of $[M + NH_4]^+$ ions of TAGs and the resultant diacyl product ions were investigated using deuterium labeling and MS/MS and MS^3 experiments. TAGs were found to undergo simple rearrangement processes to eliminate specific neutrals and generate a number of characteristic fragment ions in the MS/MS and MS^3 spectra. MS/MS was used in the analysis of TAGs to determine possible TAG molecular species present in a complex mixture without prior HPLC purification. The use of MS^3 experiments allowed for more complete and unambiguous TAG assignments to be made and led to the unequivocal identification of 54 TAG molecular species directly from a small subset of the total number of $[M + NH_4]^+$ ions derived from a complex mixture of neutral lipids extracted from RAW 264.7 cells.

Acknowledgments

This work was supported in part by the Lipid Maps Large Scale Collaborative Grant from General Medical Sciences (GM069338).

Table 8. Summary of triacylglycerol molecular species in RAW 264.7 cells ($[M + NH_4]^+$ from *m/z* 820 to *m/z* 840)

	TAG 48:0	TAG 48:1	TAG 48:2	TAG 49:0	TAG 49:1	TAG 49:2
Major	16:0/16:0/16:0	16:0/16:0/16:1	16:0/16:1/16:1	16:0/16:0/17:0	15:0/16:0/18:1	15:0/16:1/18:1
					16:0/16:1/17:0	16:0/16:1/17:1
					16:0/16:0/17:1	16:1/16:1/17:0
Minor	14:0/16:0/18:0	14:0/16:0/18:1	14:0/16:1/18:1	15:0/16:0/18:0	14:0/17:0/18:1	15:1/16:0/18:1
	15:0/16:0/17:0	14:0/16:1/18:0	14:0/16:0/18:2		15:0/16:1/18:0	
		15:0/16:1/17:0	15:0/16:1/17:1			
		15:0/16:0/17:1				
		15:0/15:0/18:1				
Trace	15:0/15:0/18:0	14:0/17:0/17:1	12:0/18:1/18:1	12:0/17:0/18:0	13:0/16:0/20:1	13:0/16:0/20:2
	12:0/18:0/18:0	14:1/17:0/17:0	14:0/17:1/17:1	13:0/18:0/18:0	14:0/16:0/19:1	14:0/15:0/20:2
	14:0/17:0/17:0	15:1/16:0/17:0	14:1/16:0/18:1	14:0/16:0/19:0	14:0/17:1/18:0	14:0/17:1/18:1
			15:0/15:0/18:2	15:0/15:0/19:0	14:1/17:0/18:0	14:0/17:0/18:2
			15:0/15:1/18:1		15:0/15:0/19:1	14:1/17:0/18:1
			15:1/16:0/17:1		15:1/16:0/18:0	15:0/16:0/18:2
			14:1/17:0/17:1			15:0/17:1/17:1
						15:1/17:0/17:1

References

1. Coleman, R. A.; Lee, D. P. Enzymes of triacylglycerol synthesis and their regulation. *Prog. Lipid Res.* **2004,** *43,* 134–176.
2. Salter, A. M.; Brindley, D. N. The biochemistry of lipoproteins. *J. Inherit. Metab. Dis.* **1988,** *1,* 4–17.
3. Gibbons, G. F. Related Assembly and secretion of hepatic very low density lipoprotein. *Biochem. J.* **1990,** *268,* 1–13.
4. Yeaman, S. J. Hormone-sensitive lipase—new roles for an old enzyme. *Biochem. J.* **2004,** *379,* 11–22.
5. Weiss, R.; Dziura, J.; Burgert, T. S.; Tamborlane, W. V.; Taksali, S. E.; Yeckel, C. W.; Allen, K.; Lopes, M.; Savoye, M.; Morrison, J.; Sherwin, R. S.; Caprio, S. Obesity and the metabolic syndrome in children and adolescents. *N. Engl. J. Med.* **2004,** *350,* 2362–2374.
6. Goodpaster, B. H.; Wolf, D. Skeletal muscle lipid accumulation in obesity, insulin resistance, and type 2 diabetes. *Pediatr. Diabetes* **2004,** *5,* 219–226.
7. Large, V.; Peroni, O.; Letexier, D.; Ray, H.; Beylot, M. Metabolism of lipids in human white adipocyte. *Diabetes Metab.* **2004,** *30,* 294–309.
8. Liu, P.; Ying, Y.; Zhao, Y.; Mundy, D. I.; Zhu, M.; Anderson, R. G. Chinese hamster ovary K2 cell lipid droplets appear to be metabolic organelles involved in membrane traffic. *J. Biol. Chem.* **2004,** *279,* 3787–3792.
9. Murata, T. Analysis of triglycerides by gas chromatography/chemical ionization mass spectrometry. *Anal. Chem.* **1977,** *49,* 2209–2213.
10. Murata, T.; Takahashi, S. Analysis of triglyceride mixtures by gas chromatography-mass spectrometry. *Anal. Chem.* **1973,** *45,* 1816–1823.
11. Hites, R. A. Mass spectrometry of triglycerides. *Methods Enzymol.* **1975,** *35,* 348–359.
12. Sjovall, O.; Kuksis, A.; Marai, L.; Myher, J. J. Elution factors of synthetic oxotriacylglycerols as an aid in identification of peroxidized natural triacylglycerols by reverse-phase high-performance liquid chromatography with electrospray mass spectrometry. *Lipids* **1997,** *32,* 1211–1218.
13. Duffin, K. L.; Henion, J. D.; Shieh, J. J. Electrospray and tandem mass spectrometric characterization of acylglycerol mixtures that are dissolved in nonpolar solvents. *Anal. Chem.* **1991,** *63,* 1781–1788.
14. Hvattum, E. Analysis of triacylglycerols with nonaqueous reversed-phase liquid chromatography and positive ion electrospray tandem mass spectrometry. *Rapid Commun. Mass Spectrom.* **2001,** *15,* 187–190.
15. Holcapek, M.; Jandera, P.; Zderadicka, P.; Hruba, L. Characterization of triacylglycerol and diacylglycerol composition of plant oils using high-performance liquid chromatography-atmospheric pressure chemical ionization mass spectrometry. *J. Chromatogr. A* **2003,** *1010,* 195–215.
16. Han, X.; Gross, R. W. Quantitative analysis and molecular species fingerprinting of triacylglyceride molecular species directly from lipid extracts of biological samples by electrospray ionization tandem mass spectrometry. *Anal. Biochem.* **2001,** *295,* 88–100.
17. Hsu, F. F.; Turk, J. Structural characterization of triacylglycerols as lithiated adducts by electrospray ionization mass spectrometry using low energy collisionally activated dissociation on a triple stage quadrupole instrument. *J. Am. Soc. Mass Spectrom.* **1999,** *10,* 587–599.
18. Byrdwell, W. C.; Neff, W. E. Dual parallel electrospray ionization and atmospheric pressure chemical ionization mass spectrometry (MS), MS/MS, and MS/MS/MS for the analysis of triacylglycerols and triacylglycerol oxidation products. *Rapid Commun. Mass Spectrom.* **2002,** *16,* 300–319.
19. Cheng, C.; Gross, M. L.; Pittenauer, E. Complete structural elucidation of triacylglycerols by tandem sector mass spectrometry. *Anal. Chem.* **1998,** *70,* 4417–4426.
20. Bligh, E. G.; Dyer, W. J. A rapid method of total lipid extraction and purification. *Can. J. Biochem. Physiol.* **1959,** *37,* 911–917.
21. Kaluzny, M. A.; Duncan, L. A.; Merritt, M. V.; Epps, D. E. Rapid separation of lipid classes in high-yield and purity using bonded phase columns. *J. Lipid Res.* **1985,** *26,* 135–140.
22. Hamilton, J. G.; Comai, K. Separation of neutral lipids and free fatty acids by high-performance liquid chromatography using low wavelength ultraviolet detection. *J. Lipid Res.* **1984,** *25,* 1142–1148.
23. Stuebiger, G.; Pittenauer, E.; Allmaier, G. Characterization of castor oil by on-line and off-line nonaqueous reverse-phase high-performance liquid chromatography-mass spectrometry (APCI and UV/MALDI). *Phytochem. Anal.* **2003,** *14,* 337–346.